Lawrence Berkeley National Laboratory
Recent Work

Title
Corrosion of Carbon Black Anodes in Alkaline Electrolyte IV

Permalink
https://escholarship.org/uc/item/9g17t3sz

Journal
Journal of the Electrochemical Society, 136(12)

Authors
Staud, N.
Sokol, H.
Ross, P.N.

Publication Date
2017-12-05

Lawrence Berkeley Laboratory

UNIVERSITY OF CALIFORNIA

Materials & Chemical Sciences Division

The Corrosion of Carbon Black Anodes in Alkaline Electrolyte: IV. Current Efficiencies for Oxygen Evolution from Metal Oxide Impregnated Graphitized Furnace Blacks

N. Staud, H. Sokol, and P.N. Ross, Jr.
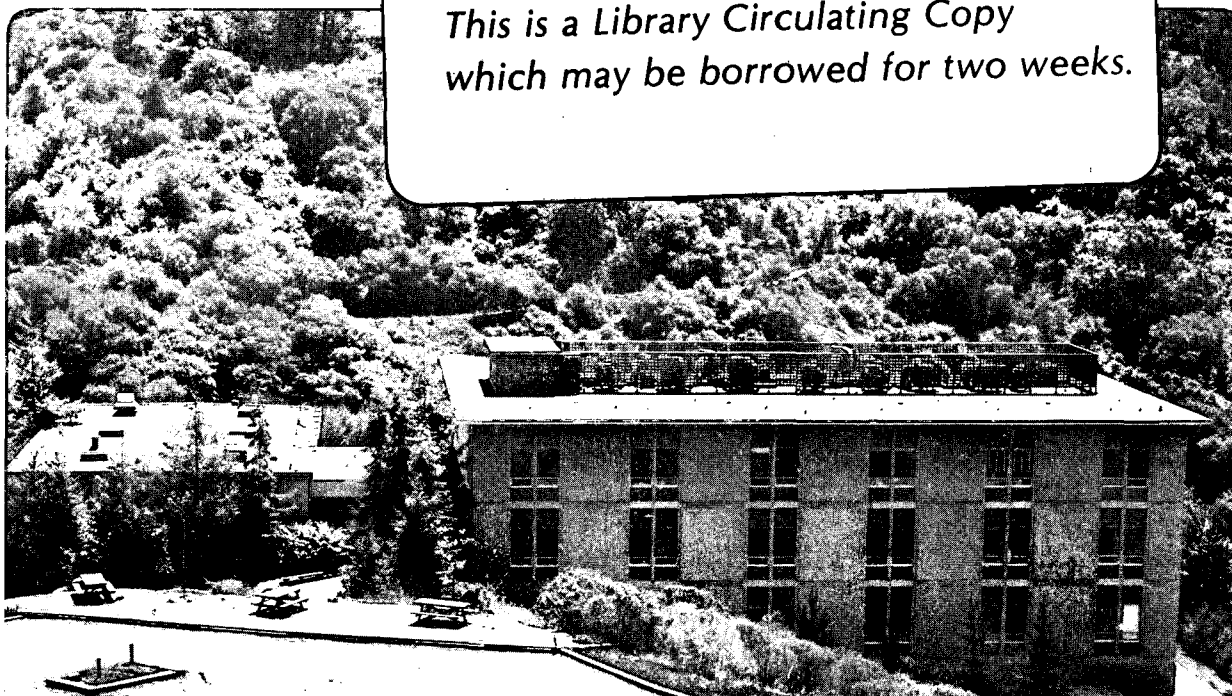
March 1989

LBL-26927

DISCLAIMER

THE CORROSION OF CARBON BLACK ANODES IN ALKALINE ELECTROLYTE

IV. Current Efficiencies for Oxygen Evolution from
Metal Oxide Impregnated Graphitized Furnace Blacks

Norbert Staud[*] , Harvey Sokol and Philip N. Ross, Jr.

Lawrence Berkeley Laboratory
Materials and Chemical Sciences Div.

Berkeley, CA 94720

Abstract

A quantitative method for determining the number of oxygenated carbon atoms in a carbon black sample was developed and applied to the study of oxygen chemisorption on graphitized furnace blacks. It was found that chemisorption of oxygen atoms produced in a low pressure microwave discharge of argon/oxygen results in the formation of an oxygen complex on every carbon atom exposed on the edge plane surface of these carbons. These combined procedures were then used to titrate the surfaces of a variety of graphitized furnace blacks for the number of edge atoms. The corrosion rate of these carbons was found to be directly proportional to the number of sites titrated by oxygen atom chemisorption, i.e. the number of edge atoms. The number of edge atoms exposed on the surface of graphitized furnace blacks depends on the microstructure of the precursor carbon black and the conditions of graphitization. Catalyzation of these graphitized carbons by NiO has little or no effect on their corrosion rate, which results in current efficiencies for oxygen evolution greater than 98%. The absence of an effect of NiO on the corrosion rate is attributed to the specificity of the corrosion reaction to edge plane sites and an apparent necessity for contact between NiO particles with edge plans for catalyzation of the corrosion reaction by NiO. NiO particles sitting on basal planes, which compose at least 90% of the surface area in these carbons, catalyze only the oxygen evolution reaction.

---

[*]Present address: IBM Magnetic Recording Institute, Almaden Research Center, San Jose, CA, 95120-6099

Introduction

In Part III (1) we reported a study of the effect of a graphitizing heat treatment on the corrosion resistance of a variety of furnace black carbons. Graphitization of a furnace black was found to significantly increase the anodic corrosion resistance, as expected from the comparable effect graphitization has on the "dry" oxidation resistance of carbon blacks (12). An analysis of different graphitized blacks appeared to indicate that corrosion resistance correlated with the number of edge plane sites exposed, some fraction of these sites possibly acting as the points of initiation of corrosive attack. It was shown that one particular type of furnace black, semi-reinforcing (SRF), having the (rubber) Industry Classification N774, is an especially good precursor for the formation of a highly graphitized and very corrosion resistant carbon black. The unique corrosion resistance of this material appeared to be associated with the unusually low number of edge plane sites on its surface. In the present work, we developed a quantitative analytical method for determining the amount of oxygen on carbon surfaces, and used this method to develop a correlation between corrosion resistance of graphitized carbons and oxygen chemisorption. Two types of oxygen chemisorption were studied, the relatively slow adsorption of oxygen from molecular oxygen and the rapid adsorption from atomic oxygen generated in a microwave discharge. The latter method appears to titrate all the carbon atoms that are exposed at the edge plane surfaces, and thus serve as a rational measure of the maximum number of active sites for corrosion of graphitized carbons. We report further on the corrosion resistance of this material when it is catalyzed with oxygen evolution catalysts and used as an oxygen evolving anode. It is shown that the current efficiency for oxygen evolution on these materials is in excess of 98%, far superior to that obtained previously with catalyzed acetylene black (2), and certainly high enough for practical application in bifunctional air electrodes (4).

Experimental

Materials – The furnace carbon blacks used in this study were obtained either from Cabot an SRF furnace black sold by Cabot under the brand name Sterling R having the Industry Classification N774 or

from Ashland Chemical (according to the Industry Classification given in Table I) and graphitized according to the procedure described previously (1). For convenience, we shall refer to the graphitized Sterling R carbon subsequently in the text as "GSR carbon". KOH electrolyte was prepared from reagent grade KOH pellets (J.T. Baker) and triply distilled water to a concentration of 30%.

Cells and electrodes – The corrosion cell used here was the same as the one used previously (2,3). The electrodes used for current efficiency measurements were prepared using the same procedure as before (2), but the procedure for catalyzing GSR carbon black with Co_3O_4 and NiO was different. The GSR carbon as-prepared is extremely hydrophobic, and thus difficult to catalyze via impregnation from aqueous solution. Instead, the impregnations were made from non-aqueous solution, using the acetate salts dissolved in methanol, followed by vacuum drying and air calcining for 2 hrs. at 300 C. As before, the current efficiency for oxygen evolution was determined using quantitative analysis of the composition of the gas above the anolyte with a mass spectrometer (1).

Microwave cavity design – The surfaces of carbon blacks were treated with atomic oxygen by exposure to an oxygen plasma created by microwave discharge. The apparatus for the microwave cavity is shown in Figure 1. The cavity was the Broids type (Opthos Instruments) operated at 2450 MHz and 50 watts. The quartz sample tube was 1.2 cm in diameter and 40 cm long, and the sample loading was typically 50–100 mg in the form of a "plug" packed between quartz wool retainers located ca. 5m downstream from the discharge cavity. The oxygen source was a high purity (Matheson Ultra-Pure Grade) mixture of 10 % oxygen in argon, with the discharge operated at 1 torr at a flow of 340 cc/min. The discharge was initiated with a Tesla coil, and continued for typically 1–4 hrs.

Thermal desorption mass spectrometer system - The absolute number of oxygen atoms on the carbon surface was determined by thermal desorption mass spectroscopy (TDMS). A schematic diagram for the TDMS system is shown in Figure 2. The sample holder was made of quartz tubing 30 cm long by 1.3 cm diameter drawn into a 2.5 cm diameter sphere at the end for sample containment. The sample gas manifold was stainless steel. The electronic manometer was a Type 221M from MKS Instruments,

3

having .01% accuracy in the 10 torr (max.) range. The mass spectrometer was a Model 100C from UTI Instruments equipped with a thoriated iridium filament ionizer and an electron multiplier detector. The computer was an IBM PC-XT with a Labmaster D/A board (Techmar). The mass spectrometer was calibrated for quantitative (volume percent) analysis of a gas containing CO, CO_2, H_2, and H_2O using calibrated gas mixtures. The absolute volume of the manifold, and thus the absolute calibration of the instrument for the above gases, was obtained by the thermal decomposition of pure compounds to produce gases in stoichiometric amounts, e.g. decomposition of formic acid to CO_2 and H_2.

The procedure for the analysis of the oxygen content of the surface of carbons was as follows. The weighed sample was put into the quartz holder and retained with quartz wool, then the holder was mounted onto the manifold. The manifold and sample holder (now containing air) were evacuated to 0.2 torr then backfilled to atmospheric pressure with argon, this sequence repeated three times. The manifold itself was outgassed by evacuation to 1.5×10^{-7} while heating the manifold, sample valve and quadrupole head to 200°C for 6 hrs. After this bakeout of the manifold, the sample was evacuated to 2×10^{-8} torr and outgassed for 2 hrs. at 100°C. Following this outgassing (to remove physisorbed gases), the sample furnace temperature ramp was started under computer control at a rate of 25°C/min. up to approximately 500°C, then progressively slower at higher temperature. From 800–1000°C the rate was 2°C/min. The absolute pressure in the manifold was recorded continuously by the electronic manometer. Composition analysis by the mass spectrometer was made periodically at selected temperatures by opening the sampling valve and admitting a differential (relative to the amount of gas in the manifold) amount of gas into the quadrupole analyzer.

Results

Oxygen content of the surface – GSR carbon is prepared by heat treatment of Sterling R carbon black at 2700°C in an inert (helium) or vacuum atmosphere. Such a high temperature treatment would in principle eliminate all the oxygen (both surface and bulk forms) from this material, so that any oxygen observed on the surface of this carbon might be presumed to come from reaction of the heat treated

4

surface to the ambient air. The thermal desorption analyses of GSR carbon showed results which are consistent with this expectation. The thermal desorption scan (referred to hereafter as TDS) for the as-prepared GSR carbon is shown in Figure 3. The principle gas given off was CO, to the extent of 12 μmols/g carbon. While still in vacuum, the sample was then cooled back to 100°C, and the analysis repeated. The only gases observed then were methane and hydrogen, in about the same quantities as observed from the as-prepared sample. The carbon was then removed from the TDS apparatus at ambient temperature, stored in a dessicator for a variable length of time, from five days up to 127 days, then a repeat analysis was made. As shown by the results reported in Figure 4, the principal gas was again CO, with the total amount increasing with time of exposure to (dry) air until saturation after about 127 days, the saturation amount being again about 12 μmols/g. The reaction of the vacuum degassed surface with air also appears to result in some states that produce CO_2 evolution in TDS, but only about 10% of the oxygen on the surface appears to be in that state. Note that both methane and CO_2 decrease in intensity above ca. 700°C. This is due to decomposition reactions within the sample holder at these temperatures, the thermodynamically most probable reactions (13) being

$$CO_2 + C ==> 2\,CO \qquad\qquad [1]$$

and

$$CH_4 ==> C + 2\,H_4 \qquad\qquad [2]$$
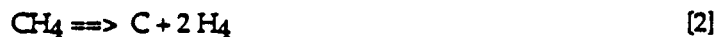
A summary of the TDS analysis of the gas evolution from a number of graphitized furnace blacks is given in Table II, along with values for three other selected carbon blacks, the GSR precursor Sterling R, acetylene black, the subject material in our previous studies (1-3), and Graphon, graphitized Spheron 6, a classical graphite material with well-studied properties of interest to this study. The number of surface carbon atoms that react with molecular oxygen in air to form adsorbed states of oxygen which thermally decompose to CO and/or CO_2 is reported as a percentage of all carbon present in the material. Also reported in Table II is the number of surface carbon atoms that react with atomic oxygen to form adsorbed states which thermally decompose to CO and/or CO_2. Figure 5 shows the TDS curves for GSR exposed to the oxygen microwave generated plasma. Note that CO_2 is now a major product,

5

evolving in roughly equal amounts to CO, at that the desorption temperatures are much lower than for CO from the GSR surface exposed only to (dry) air. These results also demonstrate more dramatically the high temperature reaction of the CO_2 evolved at lower temperatures with the carbon surface to form CO, according to eqn. [1]. The approximately equimolar ratio of CO/CO_2 was observed for all the carbons listed in the Table, and may be characteristic of the reaction of atomic oxygen with any carbon surface. Note also the evolution of significant amounts of H_2 from the plasma treated GSR, whereas H_2 was essentially undetectable from the (dry) air reacted surface. We suggest this H_2 was produced by reaction of the carbon surface with atomic hydrogen generated in the plasma due to water (impurity) in the gas delivered to the generator.

Also given in Table II is the characteristic corrosion rate of the various carbons under conditions of oxygen evolution, as measured using the same method as in Part II (2). In the potential region of interest in these studies, e.g. +400 - 650 mV vs. Hg/HgO, the corrosion rates for the three different classes of carbons studied, SRF furnace blacks, graphitized furnace blacks, and acetylene black, did not exhibit a significantly different potential dependance or a different temperature dependance. Thus, the conditions chosen for comparison of the corrosion resistance of different carbons does not depend significantly on the potential or temperature selected (within the range of potentials and temperatures of interest here). The corrosion rates in the Table are reported as the percentage of all carbon present which is dissolving per unit time. As we noted in the previous study of the corrosion resistance of graphitized carbons (3), the corrosion rates are not well correlated by BET area, which is again evident in the results in Table II, e.g. graphitized N242 and Graphon have the nearly the same BET area, but the corrosion rate of the former is six times higher. Under the conditions of oxygen exposures described above, the amount of CO or CO_2 evolving from the surface of a particular sample was quantitatively reproduced (+ 10%) upon sequential oxygen exposure and TDS analysis. For example, after the TDS analysis of a GSR sample treated with air for 120 days, the sample was cooled, and exposed again to air for (another) 120 days, and the TDS repeated with a result quantitatively the same as the initial result for the air-exposed as-prepared GSR, e.g. 12 μmols/g of CO evolved. This sequence could be repeated at least three times, but we did not explore the upper limit to the number of times this could be

6

done without changing the amount of CO produced. In the case of the oxygen plasma treatment, as long as the exposure to the plasma was not excessive, i.e. the weight loss after exposure was less than ca. 10%, the sample after TDS analysis could be exposed to air and reanalyzed with a result comparable to the initial air exposed result, i.e. the reactivity of the surface to molecular oxygen was not changed by the reaction with atomic oxygen and subsequent thermal decomposition of the surface groups.

In Part III (1), we discussed the complex time dependent behavior of the current transient from any carbon black electrode following an anodic potential step. Briefly restated here for continuity, there are two time domains to the current, one on the scale of minutes, where the current drops exponentially in time, and another on the order of hours, where the current reaches a quasi-steady state value. The corrosion rates reported in Table II are the values obtained in the latter time regime, and correspond (primarily) to the continuous dissolution of carbon to carbonate ion, whereas the initial transient period corresponds (primarily) to charge passed in surface oxidation. The distinction between these regimes is diminished at higher potentials. There appears to be a saturation level of surface oxidation which is reached more rapidly at higher potentials, but is the same level of charge at all potentials in the potential region of interest here, e.g. 400–650 mV. Based on coulometric and partial current analysis (1-3), we had estimated this saturation level to be ca. 100 $\mu C/cm^2$ (BET) (1).

In this study, we were able to confirm this charge saturation model of the behavior of carbon blacks in the transient period by independent measurements of the oxygen content of the surface using the TDS analysis. Figure 5 shows the TDS curves for GSR carbon at the end of the transient period following a potential step to 550 mV in 30% KOH at 50°C. The amount of CO_2 evolving from the surface was 28 μmols/g, which corresponds to 11.2 C/g of charge passed, and the amount of CO was 95 μmols/g, corresponding to 19 C/g of charge, so the total charge passed to produce this level of surface oxidation was 30 C/g. Since the BET area of GSR carbon was ca. 30 m^2/g, the charge on a unit BET area basis was 100 $\mu C/cm^2$, exactly the value expected from our coulometric analyses of the transient periods (1). A similar value was obtained when the carbon was potentiostatted at 400 mV for 100 hrs, supporting the previous conclusion that the same saturation charge is reached at all potentials, but requires much longer times at lower potentials.

Current efficiencies for oxygen evolution — The anodic current densities and the compositions of the anodically evolved gases were measured as a function of potential for uncatalyzed GSR carbon, and GSR carbon catalyzed by nickel oxide and cobalt oxide. The experimental procedures for these measurements were exactly the same as in Part II (2). The electrodes were held at constant potential in the potential region where significant oxygen evolution occurs, e.g. above 450 mV in 30 % KOH at 55°C, after an "aging period" at a lower potential where oxygen is not evolving, e.g. 350–400 mV. Since the rate of oxygen evolution was measured by a technique which is electrochemically equivalent to coulometry, i.e. an increase in the number of moles of oxygen in the anodic gas in a finite increment of time, the total anodic current was also measured coulometrically, from the slope of the linear region of the charge vs. time curve (time being the time from stepping the potential from open-circuit to the set potential) (2). So,

$$i_{total} = Q/\Delta t, \text{ and } i_{O_2} = 4F\, W_{O_2}/\, \Delta t, \tag{3}$$

where Δt is the sampling time increment, Q is the charge passed, and W_{O_2} is the quantity of oxygen evolved. The total corrosion currents (i_{corr}) were calculated by subtraction of the measured partial anodic current for oxygen evolution (i_{O_2}) from the overall anodic current (i_{total}). Analysis of the product distribution around the electrodes (1) indicated that the corrosion processes are primarily carbon gasification to carbon monoxide (i_{CO}) and the dissolution to carbonate ($i_{CO_3^{2-}}$). As with oxygen, the partial current for CO was calculated from the measured quantity of CO (W_{CO}) in the anolyte gas appearing in time increment Δt,

$$i_{CO} = 2F\, W_{CO}/\Delta t \tag{4}$$

The rate of weight loss (k) in $\%hr^{-1}$ was calculated from the expression

$$k = \left(\frac{M}{4F} i_{CO_3^{2-}} + \frac{M}{2F} i_{CO}\right) \times 3600 \times 100 \tag{5}$$

where M is g of carbon per mol of CO_3^{2-} and per mol of CO (hence $M=12$), and $i_{CO_3^{2-}}$ and i_{CO} are expressed in A/g carbon. Substituting for $i_{CO_3^{2-}}$ the relation yields

8

$$i_{CO_3}{}^{2-} = i_{corr} - i_{CO}$$

[6]

A summary of the anodic partial current densities, current efficiencies and weight losses for both uncatalyzed and catalyzed GSR carbon is given in Table II. These results are directly comparable to the results we reported in Part II for uncatalyzed and catalyzed acetylene black (2). In comparing the uncatalyzed carbons, it is seen that the corrosion rate for acetylene black is approximately five times higher than for GSR carbon black. A much greater difference is observed when the catalyzed materials are compared. For example, the corrosion rate of carbon from NiO catalyzed acetylene black at 550 – 600 mV is 15 times higher than from NiO catalyzed GSR carbon. The current efficiency for oxygen evolution for NiO catalyzed acetylene black in this potential range is only 50 – 60% whereas it is greater than 98% for NiO catalyzed GSR. (Note, current efficiencies for oxygen evolution greater than 98% cannot be measured with accuracy by the experimental methodology used here). The carbon corrosion rates from Co_3O_4 catalyzed GSR were much lower (factor of five) than for Co_3O_4 catalyzed acetylene black, but much higher than for NiO catalyzed GSR (an order of magnitude) and consequently the NiO catalyzed GSR has a much higher current efficiency for oxygen evolution. In the potential region of practical interest in bifunctional air electrodes, 500–600 mV, NiO catalyzed GSR had the highest current efficiency of any carbon based material we have ever examined.

Discussion

Our apparatus for the thermal desorption experiments is very similar to that used by Barton and co-workers (5). Unfortunately, they did not study any of the same carbons that we have studied here, so a direct comparison of results with very similar apparatus was not possible. We were unable to obtain a sample of Spheron 6, the channel black precursor for Graphon no longer in manufacture, which was studied by Barton and co-workers. There was a previous study of TDS from acetylene black reported in the literature by Kraus (6), who reported a total oxygen content by TDS of 0.07 wt.%, in close agreement with the value 0.062 wt.% we found here.

Table III presents three different ways of normalizing the corrosion rates by three different measures of the "active" area of the carbon: by the total number of carbon atoms on the surface, calculated from the BET area; by the number of carbon atoms adsorbing oxygen from air; by the number of carbon atoms adsorbing oxygen from atomic oxygen. Because of the highly anisotropic structure of graphite, the atomic density at the surface is very dependent on the details of the surface structure, i.e. how much of the surface is edge plane and how much is basal plane. The ideal termination of the edge plane of graphite is shown in Figure 7, with the unit cell projection onto a plane perpendicular to the basal plane and parallel to the a-axis given in Figure 7b. In a $c_0 x a_0$ unit cell, only the atoms at positions designated as 1 and 2 are true surface atoms with unsaturated sp^2 bonds emerging from the basal plane. Atoms at positions 1' and 2' are not true surface atoms, since they have the same nearest neighbor configuration as a bulk atom. The surface atomic density of this ideal edge plane termination (with $c_0 = 6.70$ Å) is therefore 1.21×10^{15} atoms/cm^2, whereas the atomic density of the basal plane is 5.73×10^{15}. Since other studies of graphitized carbons like those studied here, e.g. Graphon, have shown that the surface of these carbons appears to be primarily basal plane (7), we have calculated the atomic density of the surface assuming the ideal density of 5.73×10^{15}, an assumption which we will show subsequently leads to self consistent conclusions with respect to the fractions of the total surface area surfaces having edge plane character. Conversely, we assume that the surfaces of the amorphous carbons are essentially all edge plane, with a $c_0 = 7.00$ Å (typical value from x-ray diffraction), so that the atomic densities of these surfaces was calculated assuming 1.15×10^{15} atoms/cm^2. For consistency with the other data, the total number of atoms at the surface of each carbon is reported as a percentage of all atoms in the material. When the corrosion rate, reported as a percentage of the total carbon present in the electrode that dissolves per unit time, is normalized by any of the three measures of surface concentration, the resulting number is a turn-over number (TON), the fraction of surface atoms corroded ("turned-over") per unit time, e.g. the TON resulting from normalization by surface atomic density is the fraction of all atoms on the surface which dissolve per hr. TON is a concept frequently used in catalysis (8) for the same reason we use it here, to correlate a particular type of surface site (usually a site chemisorbing a selected molecule) with reactivity. Thus, if not all atoms on the surface

10

are equally active, the TON will vary with different preparations of the surface, and that is the result we see in Table III. If all atoms adsorbing oxygen from air are equally active (for corrosion), then a single TON should result from all samples, which again is not the case for the results in Table III. There is, however, a reasonable constancy for the TON based on the number of sites adsorbing atomic oxygen, considering that the corrosion rate measurement is only reproducible to within a factor of two (3). If we assume that all edge atoms (at sites like 1 and 2 in Figure 7) adsorb atomic oxygen, while basal plane atoms do not, then we can calculate the fraction of edge atoms as the ratio of the numbers in columns 1 and 3 in Table III. This ratio indicates that Graphon and GSR have a much lower fraction of their surface as edge planes than the other graphitized furnace blacks, e.g. 4-5 % versus 8-10 %. There appears to be a distinct difference in the TON for edge plane sites between the low edge plane materials, Graphon and GSR, and the other carbons, a difference of a factor of two. This suggests either that there are twice as many sites for corrosion on the edge plane areas of the other carbons, or that all the sites on the edge planes corrode at twice the rate. As we pointed out previously (1), high resolution electron microscopy shows that GSR has more perfectly formed layer planes than in most other graphitized furnace blacks, with evidence of regions of ABA stacking, versus wavy layer planes with ABC (rotational disorder) stacking. Thus, the detailed structure of the edge plane regions of the GSR (or Graphon) surface must be different from the structure of the edge plane regions of the less well-graphitized materials. This difference in detailed structure is probably the cause of the difference in TON for edge plane sites.

It may appear at first to be surprising that a (quasi) steady state corrosion reaction, in which material is continuously removed from the surface, should be well-correlated to any measure of the properties of the original surface, such as the chemisorption of oxygen. The explanation comes from consideration of the absolute values of the TON. At the conditions of these measurements, the rates are measured in a time period of a few hours, a time period over which only a small amount of carbon is actually lost from the electrode, in most cases much less than a monolayer(!). For example, as we have presented in great detail before (3), we measured the steady state corrosion behavior of acetylene black, including a complete material balance around the electrode, with less than two hours of

11

potentiostatting at 550 mV. As the TON in Table III indicate, in this time period less 20% of the total original surface was lost, and still less than 50% of the "active" sites (defined as the sites adsorbing atomic oxygen). One is again reminded of one of the unique virtues of electrochemical measurements, the ability to measure accurately small currents corresponding to processes involving submonolayer quantities of material.

Other studies of the surface chemistry of Graphon have also determined that the edge plane area is very small. Some of these studies also used oxygen chemisorption as a measure of edge plane area (9,10), but, as Walker and co-workers later pointed out (11), the amount of oxygen adsorbed on Graphon was very dependent on the conditions of adsorption, and it was unclear whether saturation coverage was reached in any of those studies. Groszek and Andrews used the selective chemisorption of aromatic molecules to determine the edge plane area on Graphon to be 3% of the total area, in reasonable agreement with our determination from atomic oxygen adsorption of 4%. It seems likely that atomic oxygen does adsorb to saturation on the edge planes of graphitized carbons, and that this titration method is a better method for determining edge plane area than the use of molecular oxygen at any condition.

Since the corrosion measurements reported here all correspond to the loss of submonolayer amounts of material, there is a question whether the correlations reported here would be valid for long time behavior, where the entire surface has literally turned over many times. There is a question whether passivation might occur after a longer period of corrosion, or whether anodization at higher potentials than used here might produce passivation. We cannot answer these questions definitively at this time, but we have conducted a number of experiments related to them that provide some indications of the most probable answers. With respect to the validity of the TON correlation for long term behavior, we reported above that the oxygen chemisorption results could be repeated several times in sequence, each repeat being essentially a turnover of the corroding sites, and still produce the same titration for the number of active sites. Apparently the active sites reproduce themselves upon loss of the carbon atom(s) from the site, although whether reproduction could continue indefinitely is unclear, e.g. we had repeated the titration only three successive times. We have monitored the

12

corrosion of acetylene black at a constant potential of 400 mV at 50°C for a period of up to 1000 hrs., with a total weight loss of approximately five percent (removal of ca. 3 layers of carbon surface atoms) without observing any dramatic change in the rate that would be indicative of passivation.

In comparing the results of current efficiency measurements of NiO and Co_3O_4 catalyzed GSR with the previously reported (2) results for catalyzed acetylene black, several significant differences are apparent. At the same potential under the same conditions, there is a much smaller enhancement of the carbon corrosion rate by either NiO or Co_3O_4 in the case of GSR, and with NiO in particular there is almost no enhancement at all (!), i.e. the NiO only catalyzes the oxygen evolution reaction. The practical consequences of this effect are extremely important for bifunctional air electrodes, since the carbon corrosion rate is more than an order of magnitude lower with NiO catalyzed GSR carbon than with NiO catalyzed acetylene black. As we discussed before (2), the mechanism by which these metal oxides catalyze carbon corrosion is not clear, although there are several different possibilities. In the case of GSR carbon, a highly graphitized material, we can suggest an explanation for very reduced catalysis relative to acetylene black based on a physical contact mechanism. If the corrosion reaction is catalyzed by the metal oxide only at or very near the points of contact between the carbon and the metal oxide, then the highly anisotropic nature of the GSR surface, with only 5% of the surface as edge plane sites potentially active for corrosion, means that the metal oxide particles, if uniformly distributed over the carbon surface, have far fewer possible points of contact with parts of the GSR carbon surface that are (or are potentially) corroding.

Acknowledgements

References

1)   P. Ross and M. Sattler, This Journal, 135 (1988) 1464.

2)   N. Staud and P. Ross, This Journal, 133 (1986) 1079.

3)   H. Sokol and P. Ross, This Journal, 131 (1984) 1742.

4)   B. Demzyk and C. Liu, This Journal, 129 (1982) 1159.

5)   S. Barton, G. Boulton and B. Harrison, Carbon, 10 (1972) 395; J. Brown, J. Dollimore, C. Freedman
        and B. Harrison, Thermochimica Acta, 1 (1970) 499.

6)   A. Groszek and G. Andrews, Third Conference on Industrial Carbons and Graphite, Society of
        Chemical Industry, London, 1971, p. 156.

7)   G. Kraus, J. Phys. Chem. 59 (1955) 343.

8)   See Chapter 1 in M. Boudart and G. Djega - Mariadassou, "Kinetics of Heterogeneous Catalytic
        Reactive", Princeton Univ. Press, Princeton NJ, 1984..

9)   N. Laine, F. Vastola, and P. Walker, J. Phys. Chem. 67 (1963) 2030.

10)   See literature review in "Carbon: Electrochemical and Physicochemical Properties", K.
        Kinoshita, Wiley-Interscience, New York, 1988, p. 175-77.

11)   R. Lussow, F. Vastola and P. Walker, Carbon 5 (1967) 591.

12)   W. Smith and M. Polley, J. Phys. Chem 60(1956) 689.

13)   From the Thermodynamic data reported in "The Chemical Thermodynamics of Organic
        Compounds, D. Satull, E. Westrum and G. Sinke, eds., J. Wiley and Sons, New York, 1969.

Table I. Summary of Thermal Desorption (TDS) and Anodic Corrosion Rate[a] Measurements for Various Carbon Blacks

Carbon	BET Area (m^2/g)	Carbon Atoms Adsorbing Oxygen (%)[b]		Corrosion Rate (% hr^{-1})[b]
		From O_2	From O^*	
Graphitized N110	100	0.041	0.917	0.22
Graphitized N219	80	0.034	0.858	0.17
Graphilitzed N242	75	0.067	0.922	0.27
Graphitized N326	55	0.044	0.546	0.15
GSR	28	0.013	0.156	0.020
Graphon	81	0.017	0.363	0.045
Sterling R	25	0.148	0.655	0.150
Acetylene black	71	0.062	0.540	0.100

[a] at 550 mV vs Hg/HgO in 35% KOH at 50°C.
[b] % ≡ percent by weight of all carbon present

15

Table II. Correlation of Anodic Corrosion Rate with the Number of Carbon Atoms on Vacuum Degassed Carbon Blacks Adsorbing Oxygen from O_2 and/or O^*

Carbon	Carbon Atoms* on Surface (%)[b]	Carbon Atoms Adsorbing Oxygen (%)[b]		Fraction of Surface Adsorbing O^*	Normalized Corrosion Rate (TON hr^{-1})		
		From O_2	From O^*		By Surface Area	By O_2 Adsorbed	By O^* Adsorbed
Graphitized N110	11.5	0.041	0.917	7.8%	0.019	5.5	0.24
Graphitized N219	9.17	0.034	0.858	9.4%	0.018	5.0	0.20
Graphitized N242	8.60	0.067	0.922	11.6%	0.031	4.1	0.29
Graphitized N326	6.30	0.044	0.546	8.7%	0.024	3.4	0.27
GSR	3.21	0.013	0.156	4.0%	0.006	1.5	0.13
Graphon	9.20	0.017	0.363	3.9%	0.005	2.6	0.12
Sterling R	0.58	0.148	0.655	100%	0.260	1.0	0.23
Acetylene black	1.62	0.0624	0.540	33%	0.062	1.6	0.19

*calculated from BET area assuming 5.73×10^{15} atoms/cm^2 for graphites and 1.15×10^{15} atoms/cm^2 for amorphous carbons (see text)
[b]% ≡ percent by weight of all carbon present

16

Table III. Current Densities, Current Efficiencies and Corrosion Rates for Uncatalyzed and NiO and Co_3O_4 Catalyzed "Graphitized Sterling R" (GSR) Black at 55°C.

			Uncatalyzed GSR				
E (mV)	I_{total} (mA/mg)	I_{O_2} (mA/mg)	% O_2	I_{CO} (mA/mg)	% CO	I_{corr} (mA/mg)	Weight loss (% hr^{-1})
550	0.026	0.023	89	0.001	5	0.003	0.04
600	0.187	0.170	91	0.009	5	0.017	0.29
650	0.410	0.369	90	0.021	5	0.041	0.69
700	0.680	0.619	91	0.034	5	0.061	1.06

			20 w/o NiO on GSR				
E (mV)	I_{total} (mA/mg)	I_{O_2} (mA/mg)	% O_2	I_{CO} (mA/mg)	% CO	I_{corr} (mA/mg)	Weight loss (% hr^{-1})
550	0.187	0.178	95	–	–	0.009	0.10
600	1.450	1.421	>98	–	–	0.029	<0.32
650	2.971	2.912	>98	–	–	0.059	<0.66
700	4.342	4.255	>98	–	–	0.087	<0.97

			20 w/o Co_3O_4 on GSR				
E (mV)	I_{total} (mA/mg)	I_{O_2} (mA/mg)	% O_2	I_{CO} (mA/mg)	% CO	I_{corr} (mA/mg)	Weight loss (% hr^{-1})
550	0.404	0.356	88	0.020	5	0.048	0.77
600	1.854	1.687	91	0.093	5	0.167	2.91
650	4.125	2.919	95	0.124	3	0.206	3.69
700	6.470	6.341	>98	0.129	<2	0.129	2.89

17

Fig. 1   Schematic diagram of system for treating carbon black in microwave generated oxygen plasma.

Fig. 2   Schematic diagram of thermal desorption mass spectrometer system for measurement of number of mols of gas evolving from carbon blacks as a function of temperature.

Fig. 3   Thermal desorption curves for GSR carbon in the as-prepared (air equilibrated) state.

Fig. 4   Repeat of thermal desorption from GSR carbon after vacuum at 1000°C followed by air (dry) exposure for 127 days.

Fig. 5   Thermal desorption curves for GSR carbon after exposure to the microwave generated oxygen plasma (see text for conditions).

Fig. 6   Thermal desorption curves for GSR carbon after anodic oxidation in 35% KOH at 550 mV vs Hg/ Hg.0 at 50°C.

Fig. 7   a) Crystal structure of graphite; b) structure of (100) surface formed by the a - c axes indicated; 1 and 2 are atoms in the surface plane while 1' and 2' are atoms in the subsurface plane.
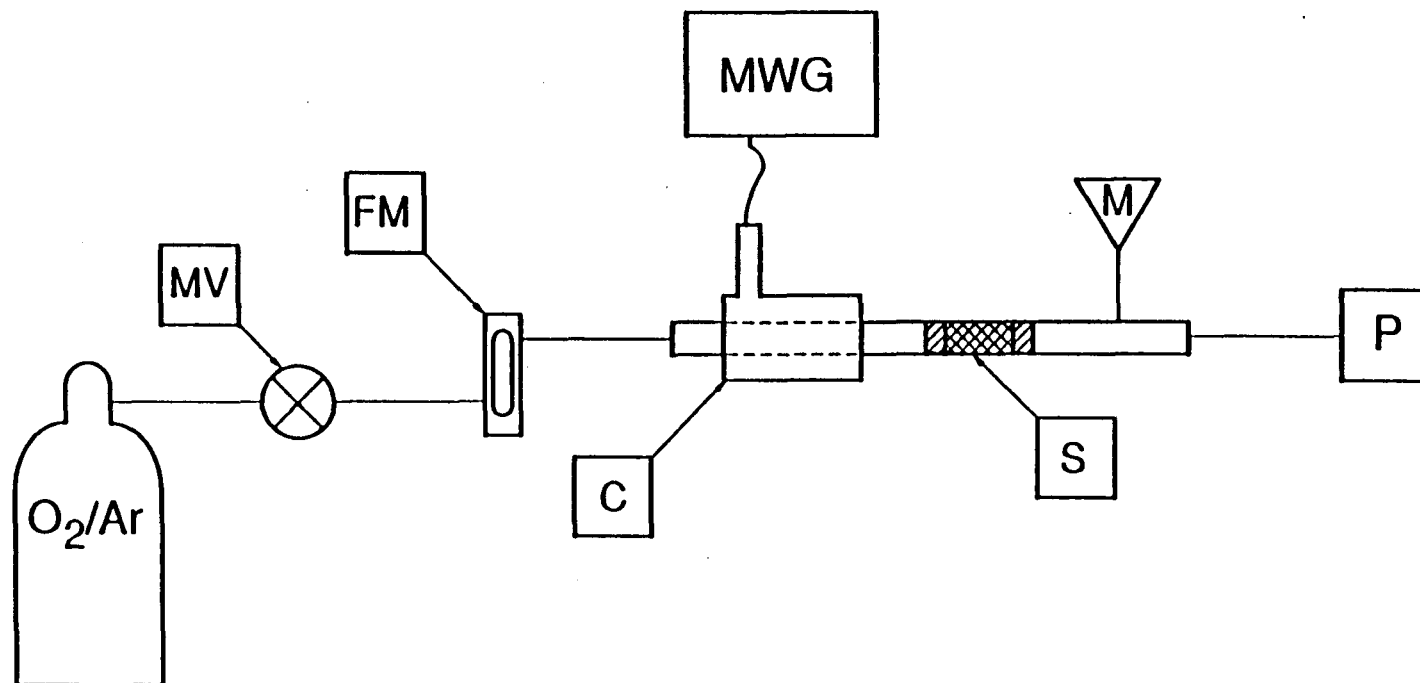
MV-fine metering valve; FM-flowmeter; MWG-microwave generator;
C-microwave cavity; M-electronic manometer; P-vacuum pump

Fig. I
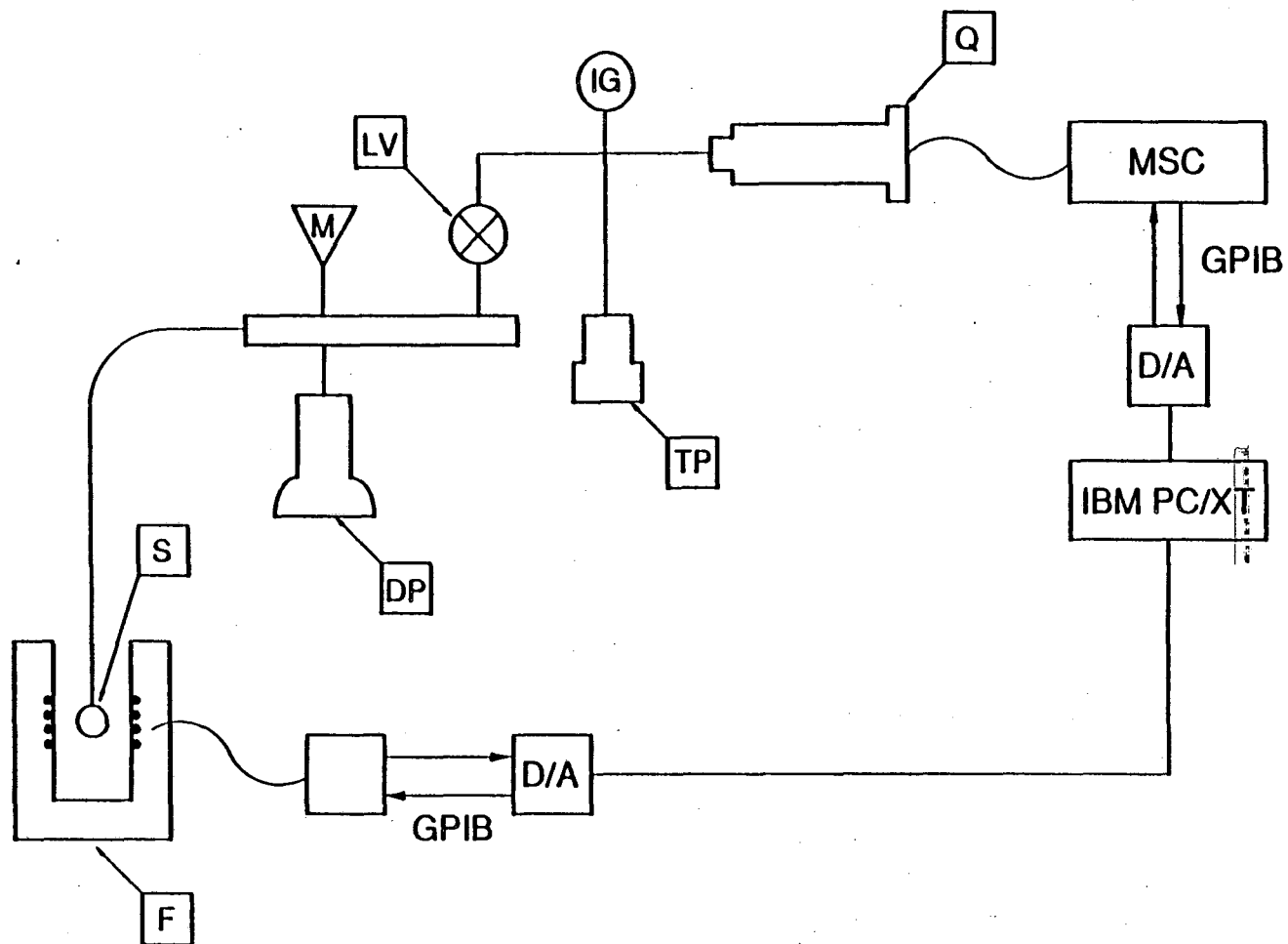
F-furnace; FC-furnace controller; S-sample holder; M-electronic manometer; DP-diffusion pump; LV-leak valve; IG-ion gauge; TP-turbomolecular pump; Q-quadrupole mass analyzer; MSC-controller
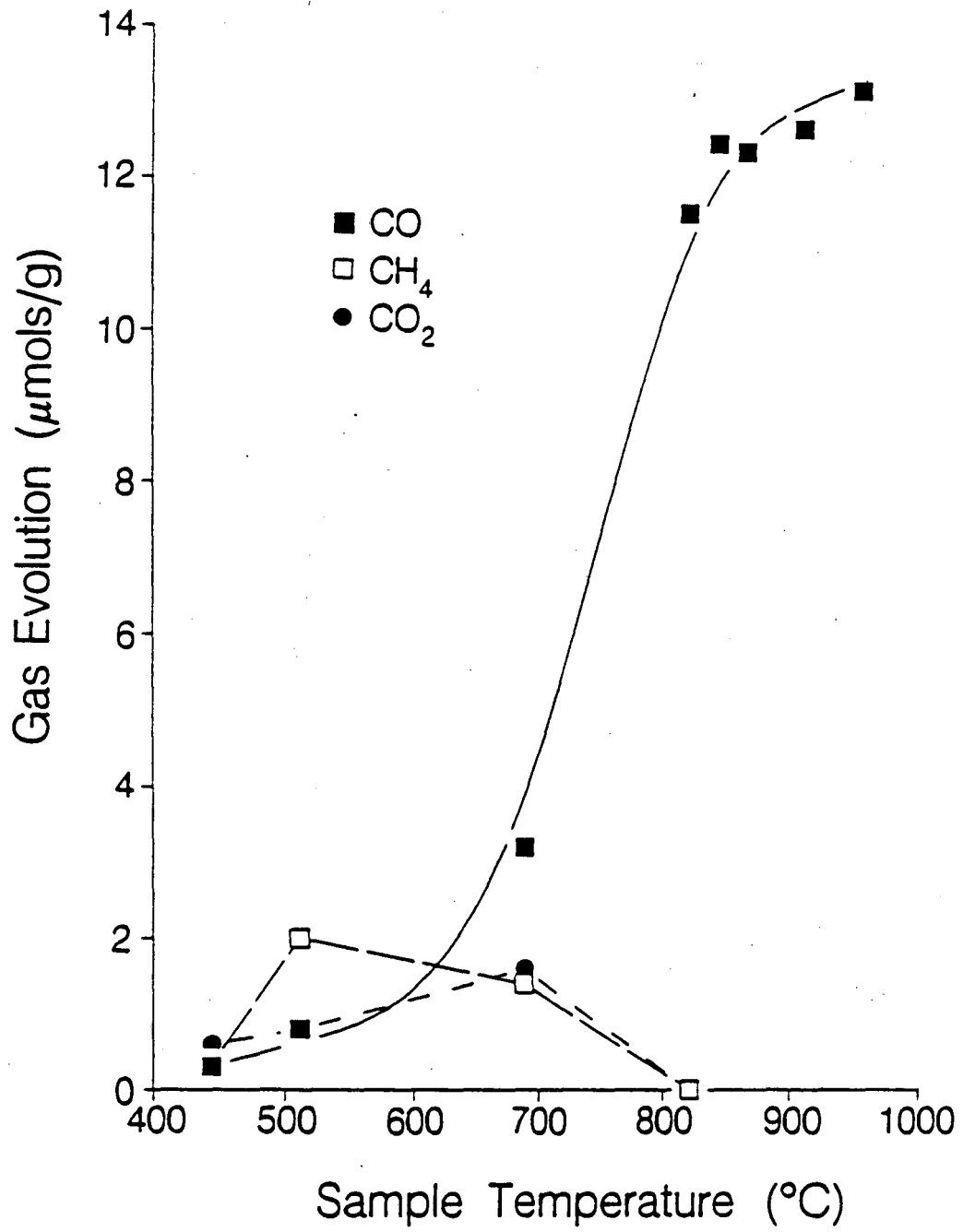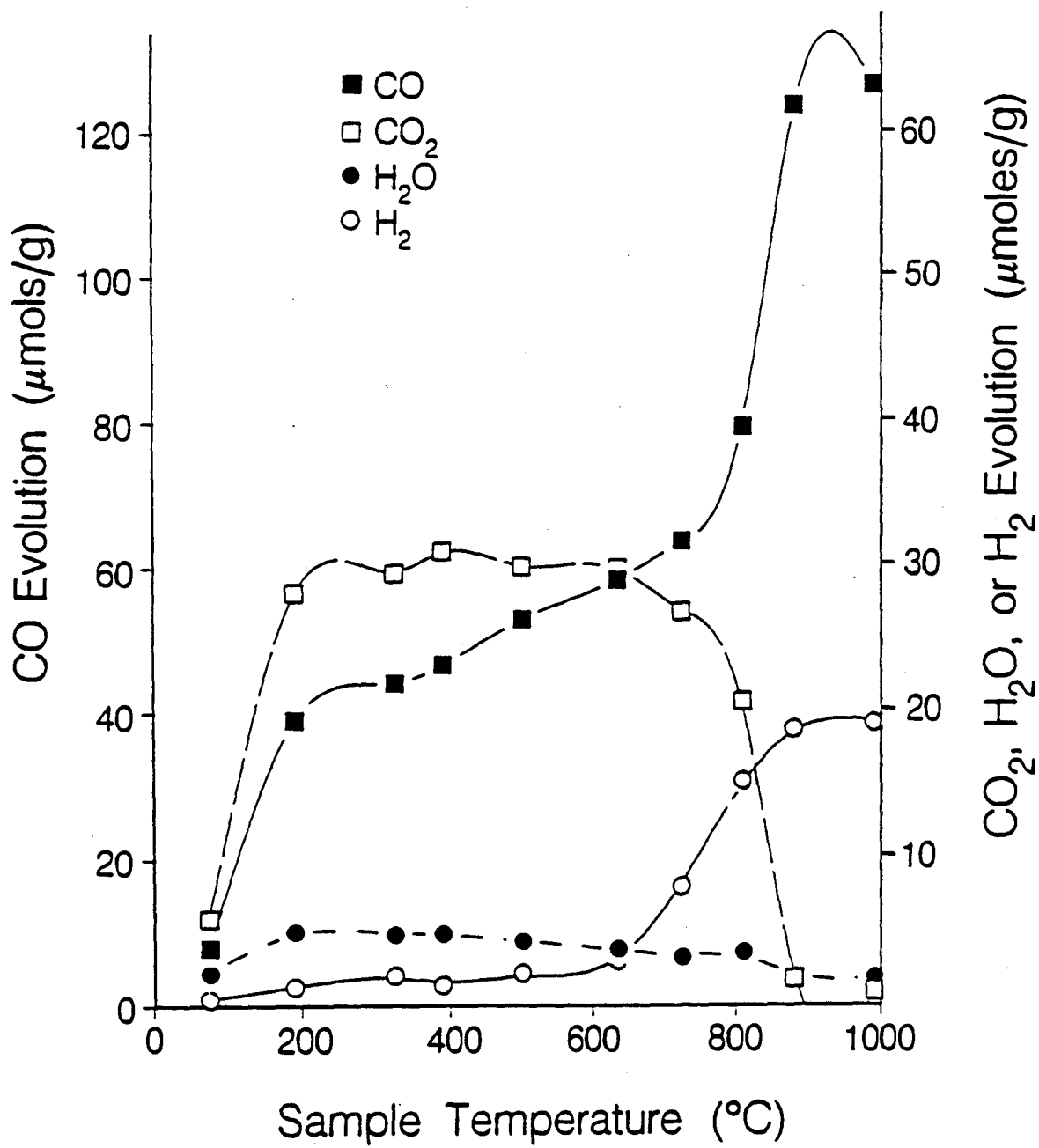
XBL 891-7409
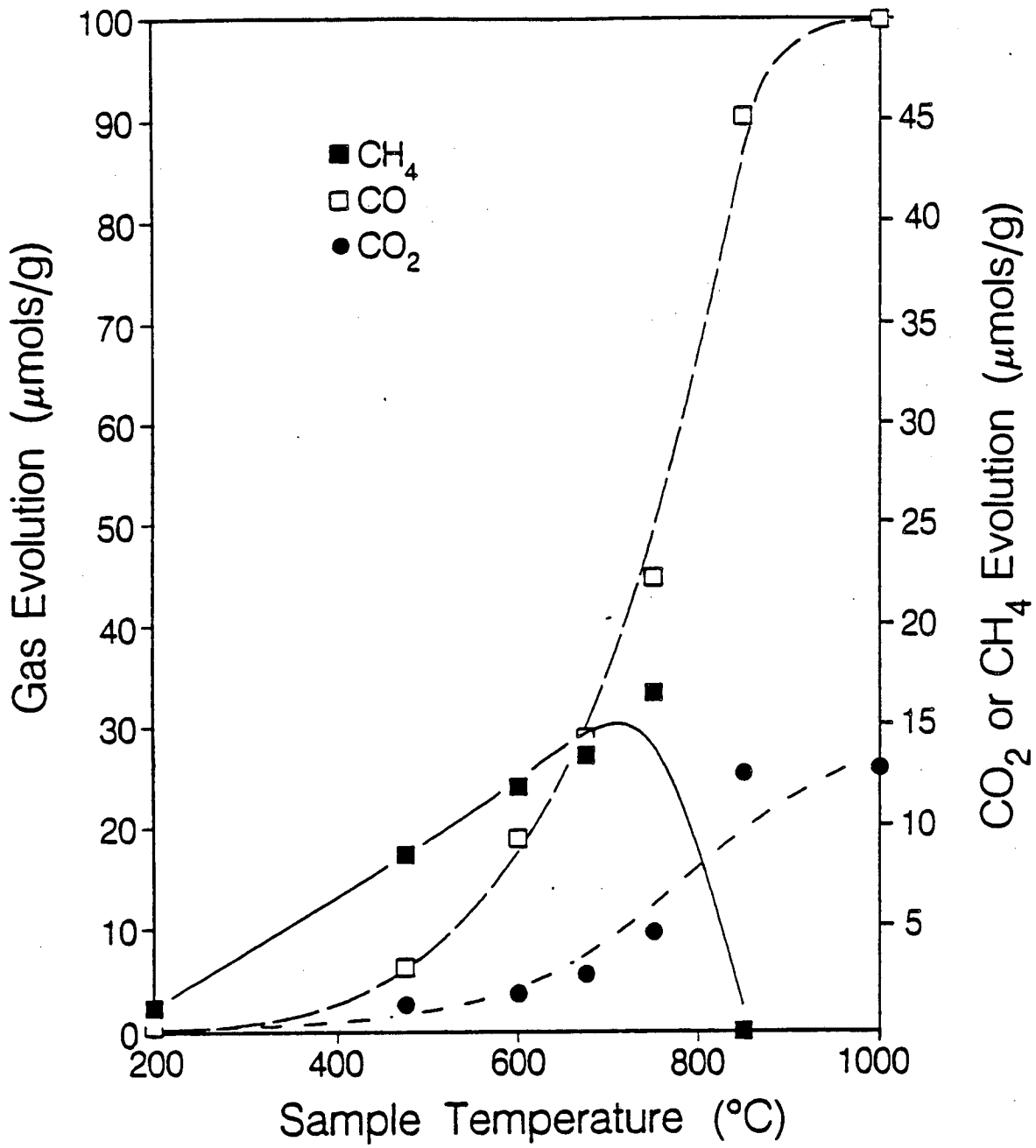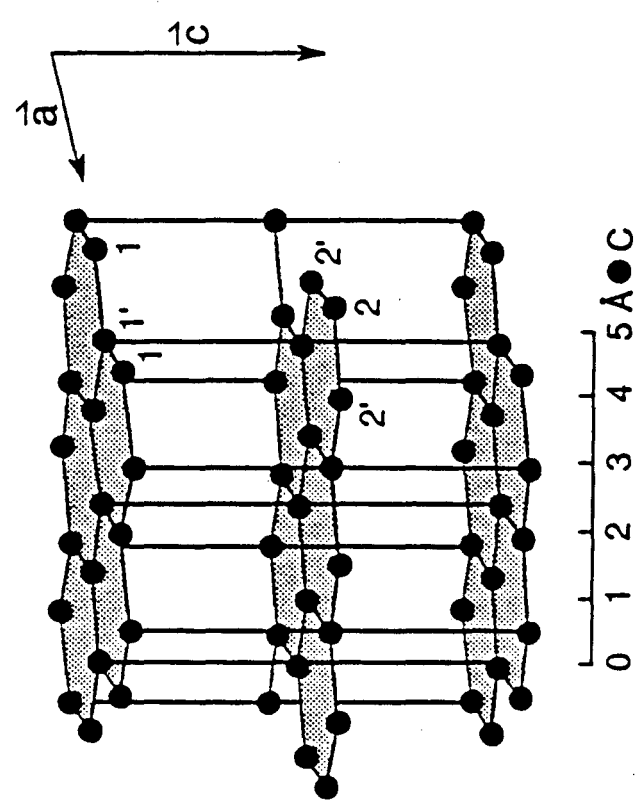
Fig. 2

XBL 891-7405

Fig. 3

21

Fig. 4

22
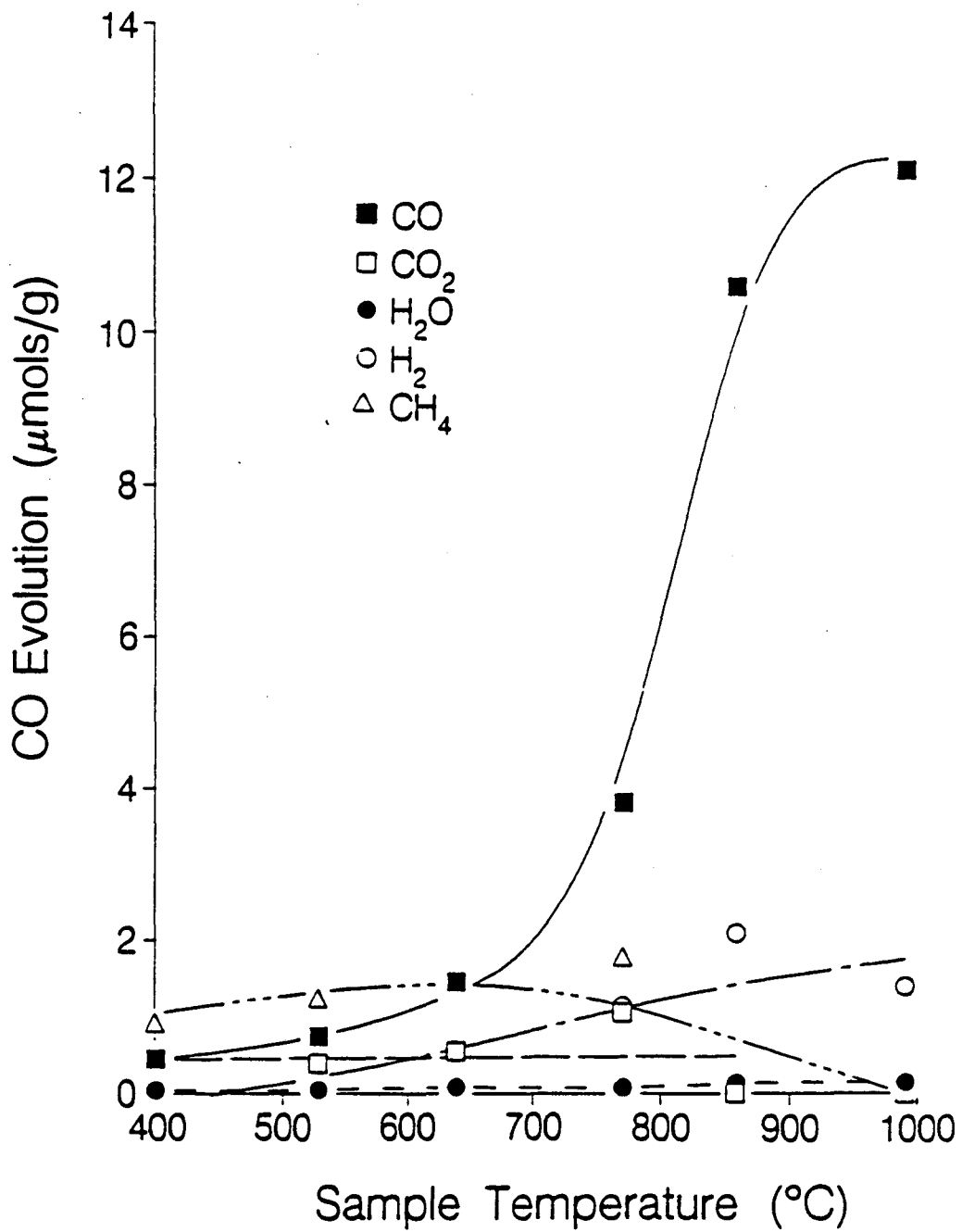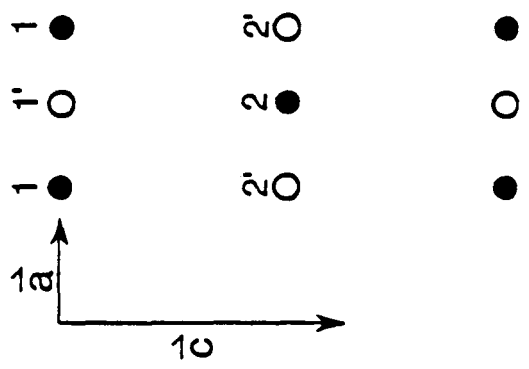
XBL 891-7408

Fig. 5

XBL 891-7407

Fig. 6

24

(a)

(b)

XBL 891-7411

Fig. 7

25